

# Finite Element Analysis of an Enzymatic Biofuel Cell: The Orientations of a Chip inside a Blood Artery

Yamini S. Parikh, Yin Song, and Chunlei Wang

Mechanical & Materials Engineering Department, Florida International University  
10555 W. Flagler St., Miami, FL 33174, USA, wangc@fiu.edu.

**Abstract:** Output performance of an implantable enzymatic biofuel cell (EBFC) with three-dimensional highly dense micro-electrode arrays has been simulated with a finite element analysis approach. The purpose of this research is to optimize the orientation of this EBFC chip inside a blood artery such that the mass transport of glucose around all the micro-electrodes can be improved and hence output performance. Based on the analysis of horizontal and vertical position of a chip, we propose a new chip design for the EBFC chip. Results show that the chip is more stable in the vertical position (VP) rather than in horizontal position (HP). In VP, the diffusive flux is uniform at top portions of all electrodes. In HP, the diffusive flux is highest at the outer electrodes while reducing almost to zero at the central electrodes. The diffusive flux has been drastically increased in a chip with holes in between the electrodes on a substrate.

**Keywords:** Finite element analysis, Enzymatic biofuel cell, Blood artery, Navier stokes equations, Orientation.

## 1. Introduction

Enzymatic Biofuel Cells (EBFCs) might be the possible next generation electrochemical power sources to supply electricity to the implantable active biomedical devices, such as pace makers, insulin pumps, cochlear implants etc [1-5]. The EBFCs use enzymes as catalysts to convert chemical energy entrapped in bio-molecules to electrical energy.

## 2. Computational Modeling

The 2-D computational models of a miniature EBFC with highly dense 3-D cylindrical micro-electrodes arrays are built to simulate the behavior in transient conditions. The EBFC chips are assumed to be centrally

located inside a blood artery, where the continuous supply of glucose and oxygen from the blood is easily accessible. On anode, the glucose is oxidized via glucose oxidase enzyme and generates gluconolactone. On cathode, dissolved oxygen is reduced via laccase enzyme and generates water by combining with electrons and hydrogen ions. Water is the only byproduct from this reaction, which prevents contamination due to metals as in case of other biofuel cells.

### 2.1 Computational geometry

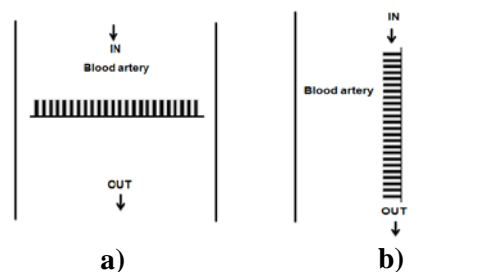


**Figure 1.** Computational geometry of different orientations of an EBFC in a) Horizontal position (HP), and b) Vertical Position (VP)

Figure 1 shows the computational geometry of the EBFC. Total 12 pairs of anodes and cathodes are accommodated on a 1 mm long SiO<sub>2</sub> insulation layer. In HP, all the electrodes are facing the inlet and in VP, all electrodes are facing the blood artery wall. The height of all electrodes is 300 μm, diameter is 30 μm, distance between two electrodes is 40 μm and the enzyme layer thickness is 10 μm. The blood vessel is assumed to be straight, rigid and having 1.5 cm diameter [6].

### 2.2 Boundary conditions

The boundary conditions are shown in table 1 and 2 for Navier Stokes and Electro-kinetics application modules, respectively. The sub-

domain properties and expressions used in the modeling are enumerated in the appendix (Table 3).

**Table 1** Boundary conditions for Navier Stokes Application module

Boundary	Condition
Anode – enzyme layer interface & Cathode – enzyme layer interface	Wall – no slip
Enzyme layers – electrolyte interface	Continuity
Inlet of an artery	Inlet pressure
Outlet of an artery	Outlet – No viscous stress
SiO <sub>2</sub> layer	Insulation

**Table 2** Boundary conditions for Electro-kinetic application module.

Boundary	Condition
Anode – enzyme layer interface, & Cathode – enzyme layer interface	Zero inward flux
Enzyme layers – electrolyte interface	Continuity
Inlet of an artery	Inward flux= 5 mM [7,8]
Outlet of an artery	Convective flux
SiO <sub>2</sub> layer boundaries	Insulation

The pressure variation at the inlet of an artery follows a function shown in figure 2. This function is multiplied by 50 mmHg at the inlet to maintain normal pressure range of 80 mmHg to 120 mmHg in the artery.

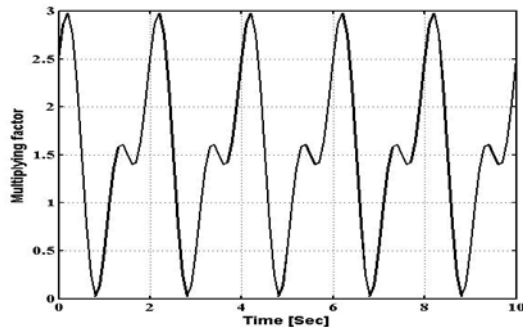


**Figure 2.** Multiplying curve for pressure at the inlet of an artery. (COMSOL fluid structure interaction in a network of a blood vessel)

### 3. Results and discussions

#### 3.1 Pressure and velocity distribution

Inside a blood artery, the pressure and velocity around the EBFC chip have been simulated and plotted as shown in figure 3. Figure 3a and 3b shows the velocity profiles for HP and VP, respectively. There are boundary layers, marked by parabolic curves, are observed at the blood artery walls and chip surfaces. The flow pattern is parabolic inside an artery, starting with zero velocity at vessel walls and gradually increasing to the center of an artery. There is a wake region (zero velocity) below the chip in a HP (figure 3a), which cannot be seen in VP (figure 3b). In HP, the angle of attack due to chip in front of the glucose flow is large compared to VP. This results in a wake region below the chip in HP. Fluid layers stick to the chip surfaces turn into random flows in this wake region which can be seen from figure 3c. The small random flow below the chip may lift up the chip. In VP (figure 3d), there are no vortices formed below the chip and the flow is mostly laminar.

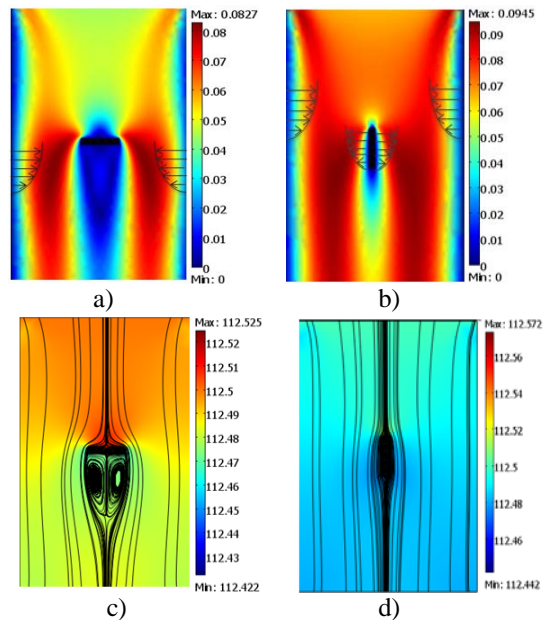


**Figure 3.** Velocity surface plot for a chip in a) HP, b) VP, and pressure surface plot with velocity streamlines for a chip in c) HP and d) VP.

As observed from the figure 3c, for HP, there is a sudden pressure change above and below the chip which can eventually push down the chip. In VP, the pressure is almost uniform around the chip. Therefore, it is easy for a chip to be stable in case of VP. In HP, the chip should be attached properly and firmly so that the chip can be sustained against the vibrations due to flow.

### 3.2 Glucose flux around micro-electrodes

We have analyzed diffusive flux and convective flux in between all micro-electrodes in horizontal as well as vertical positions. The diffusive flux is solely dominated by concentration gradient and reaction rate inside the enzyme layers, while convective flux is solely dominated by convection. Total flux is a combination of these two.

Figure 4a and 4b demonstrate the diffusive flux in between all microelectrodes for HP and VP, respectively. It is inspected that the diffusion is negligible in between electrodes for up to 200  $\mu\text{m}$  height of electrodes and then it is increasing on the top of the electrodes, in both HP and VP.

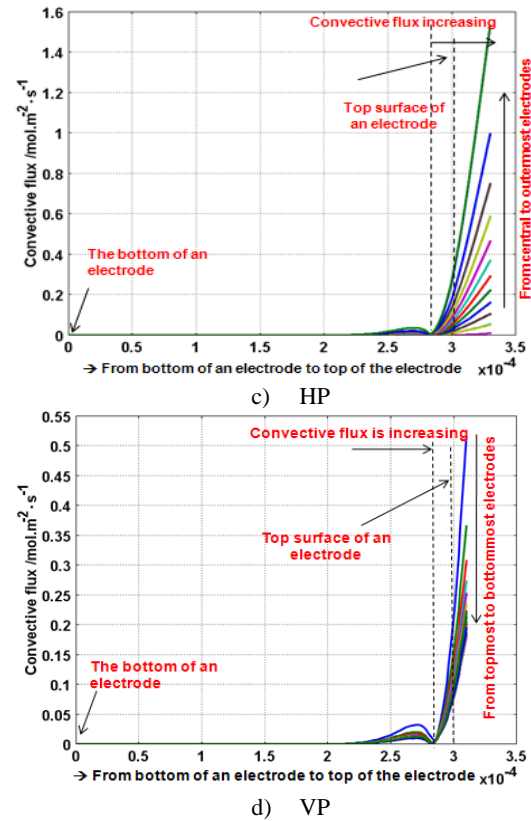
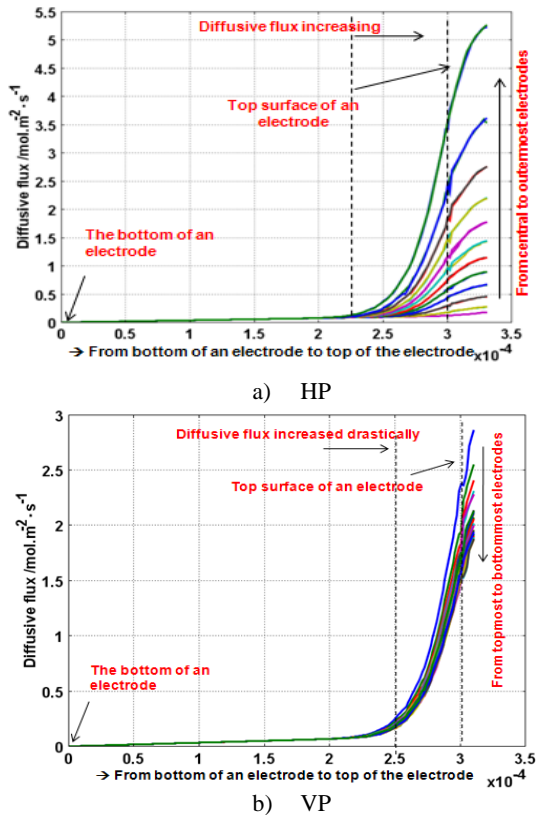


**Figure 4.** Graphical plots in between all electrodes a) diffusive flux in HP, b) diffusive flux in VP, c) Convective flux in HP, and d) convective flux in VP.

In HP, the outermost electrodes on a chip are having more diffusive flux at the top portions of the electrodes compared to central electrodes. The flux is increasing while going from inner to towards outermost electrodes. In case of VP, the flux is almost similar from uppermost electrodes to bottommost electrodes on a chip.

From figure 4a and 4b, it is inferred that the glucose diffusion in between electrodes up to 200  $\mu\text{m}$  height is almost negligible. The glucose diffusion flux is approximately  $4 \text{ mol.m}^{-2}.\text{s}^{-1}$  at the top portions of the electrodes and it is decreasing to almost zero at the center of the chips, in case of HP. In VP, diffusion flux at the top portions of the electrodes is around  $1.5 - 2.5 \text{ mol.m}^{-2}.\text{s}^{-1}$  for all electrodes.

Figure 4c and 4d illustrates the convection profiles around micro-electrodes. There is negligible convection in between all electrodes in HP as well as VP of a chip below 250  $\mu\text{m}$  height. The velocity of glucose flow is increasing

at top portions of the electrodes, while going from central to outermost electrodes (figure 3a) and hence the convection is also increasing in HP (figure 3c).

The glucose is forced to flow away from the chip in a HP and hence the convective flux is higher at the extreme ends of a chip, while reducing towards inner electrodes of a chip. In VP, the velocity is similar on top of all electrodes (figure 3b) and hence the convective flux is nearly same on top of the electrode (figure 4d) with negligible convection in between electrodes.

### 3.3 Optimized design

In above sections, it can be concluded that there is a minimum glucose diffusion and negligible convection in between electrodes. In order to improve the performance of the EBFC, it is necessary to improve the diffusion in between electrodes to utilize all enzymes in reaction and hence generate more number of electrons to achieve the output potential.

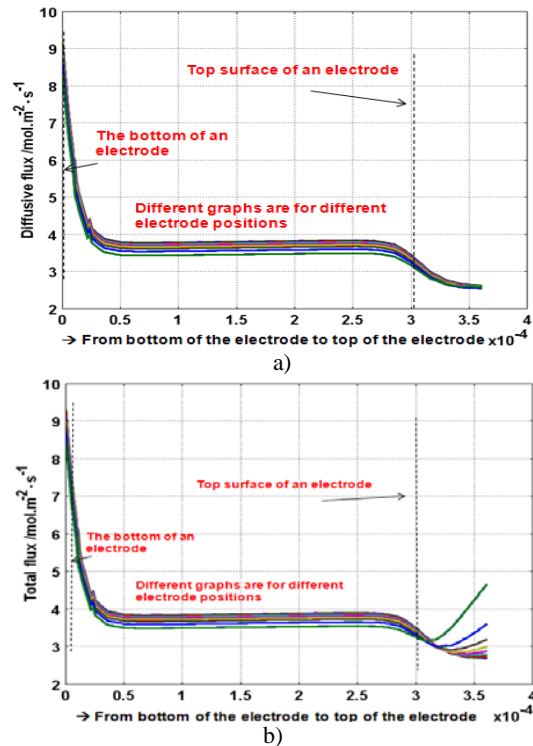


**Figure 5.** Graphical plots in between all electrodes with holes in a substrate, a) diffusive flux, and b) convective flux.

We here propose a new chip design for HP with holes in the substrates. The holes size can be varied based on the distance between two electrodes. For example, in our design we have considered holes with same diameter of 20  $\mu\text{m}$ .

The graphical representation for diffusive flux and convective flux is shown in figure 5a and 5b. The diffusive flux is enhanced in between electrodes and it is uniform from top to bottom of the electrodes. The diffusion is 4  $\text{mol.m}^{-2}.\text{s}^{-1}$  at top of all electrodes. If we compare it with the design without holes, then the diffusion has improved drastically in the new design. The convection as shown in figure 5b has not been improved compared to the chip without holes. This is because such small micron spaced holes between the electrodes cannot really provide enough space for changing the velocity of a flow. These holes can also be beneficial in preventing bubbles in gas formation or any other small particles (blood contents) to agglomerate in between electrodes.

### 4. Conclusions

From the comparison of an EBFC chip inside a blood artery with respect to different orientations- HP and VP, it can be concluded that the chip can be more stable in the VP. The diffusive flux is uniform on top of all electrodes in VP, while in HP, the flux is negligible in the center of a chip, while increasing towards outermost electrodes.

In HP, by providing holes in the substrate, we can drastically improve the diffusion in between the micro-electrodes.

### 5. References

1. X. Wei, J. Liu, Power sources and electrical recharging strategies for implantable medical devices, *Front Energy and Power Eng.* **2** 1-13 (2008)
2. L. Brunel, J. Denele, K. Servat, K. B. Kokoh, C. Jolival, C. Innocent, M. Cretin, M. Rolland, S. Tingry, Oxygen transport through laccase biocathodes for a membrane-less glucose/O<sub>2</sub> biofuel cell, *Electrochem. Commun.* **9** 331-336 (2007)
3. S. M. Venkateswara, V. Ilankumaran, N. S. Rao, *Trends in Cardiac Pacemaker Batteries,*

Indian Pacing and Electrophysiology Journal **4** 201-212 (2004)

4. E. Katz, A. F. Buckmann, I. Willner, Self-Powered Enzyme-Based Biosensors, Journal of Am. Chem. Soc. **123** 10752-10753 (2001)

5. R. A. Bullen, T. C. Arnot, J. B. Lakeman, F. C. Walsh, Biofuel cells and their development, Biosensors & Bioelectronics **21** 2015-2045 (2006)

6. C. Kleinstreuer, *Biofluid dynamics*, 479, CRC Press, Boca Raton, (2005)

7. N. Mano, A. Heller, Biofuel cells and their development, J. Electrochem. Soc. **150** A1136-A1138 (2003)

8. A. Heller, B. Feldman, Electrochemical glucose sensors and their applications in diabetes management, Chem. Rev. **108** 2482-2505 (2008)

9. N. Mano, V. Soukharev, A. Heller, A Laccase-Wiring Redox Hydrogel for Efficient Catalysis of O<sub>2</sub> Electroreduction, J. Phys. Chem. B **110** 11180-11187 (2006)

10. G. W. Albin, T. A. Horbett, S. R. Miller, N. L. Ricker, Theoretical and experimental studies of glucose sensitive membranes, J. Controlled Rel. **6** 267-291 (1987)

11. H. Li, R. Luo, E. Birgersson, K. Y. Lam, A chemo-electro-mechanical model for simulation of responsive deformation of glucose-sensitive hydrogels with the effect of enzyme catalysis, J. Mech. Phys. Solids **57** 369-382 (2009)

12. Gilles k. Kouassi, Joseph Irudayaraj, Gregory McCarty, Activity of glucose oxidase functionalized onto magnetic nanoparticles, BioMagnetic Research and Technology **3** 1-10 (2005)

13. M. Y. Ahn, A. R. Zimmerman, C. E. Martínez, D. D. Archibald, J. M. Bollag, J. Dec, Enzyme and Microbial Technology **41** 141-148 (2007)

14. E. E. Spaeth, S. K. Friedlander, The Diffusion of Oxygen, Carbon dioxide and inert gas in flowing blood, Biophysical Journal **7** 827-851 (1967)

15. N. Matsuda, K. Sakai, Blood flow and oxygen transfer rate of an outside blood flow membrane oxygenator, Journal of membrane Science, **170** 153-158 (2000)

16. F. Barriere, Y. Ferry, D. Rochefort, D. Leech, Targetting redox polymer as mediators for laccase oxygen reduction in a membrane-less biofuel cell, Electrochemistry Communications **6** 237-241 (2004)

17. F. Hirsch, E. Texter, L. Wood, W. Ballard, F. Horan, I. Wright, C. Frey, D. Starr, The Electrical Conductivity of Blood, J. American Society of Hematology **5** 1017-1035 (1950)

18. D. L. Wise, G. E. Wnek, D. J. Trantolo, T. M. Cooper and J. D. Gresser, Electrical and Optical polymer systems: Fundamentals, Methods and applications, CRC Press, New York, (1998)

19. I. Willner, E. Katz, F. Patolsky, A. F. Buckmann, Biofuel cell based on glucose oxidase and microperoxidase-11 monolayer-functionalized electrodes, J. Chem. Soc., Perkin Trans. **2**, 1817-1822 (1998)

## 6. Acknowledgements

This project is supported by national Science Foundation CBET # 0709085. We thank to Dr. Marc Madou at University of California Irvine, Dr. Sylvia Daunert at University of Kentucky, Dr. Jihua Chen and Dr. Norman Munroe at Florida International University for useful discussion.

## 7. Appendix

**Table 3** Boundary conditions for Electro-kinetic application module.

Description	Values
Universal gas constant	8.314 J.mol <sup>-1</sup> .K <sup>-1</sup>
Body Temperature	300 K
Faraday's constant	96485 C.mol <sup>-1</sup>
Diffusion co-efficient of glucose	7e-10 m <sup>2</sup> .s <sup>-1</sup> [9-11]
Michaelis Menten constant for GOx	0.383 mM [12]
Michaelis Menten constant for laccase	0.18 mM [13]
Number of electron transfer at anode	2
Normal Hematocrit value	42 %
Diffusion co-efficient of oxygen	(2.13-(0.0092*Ht))*(1e <sup>-9</sup> ) m <sup>2</sup> .s <sup>-1</sup> [14-15]
Maximum reaction rate of GOx	0.731 mM.min <sup>-1</sup> [12]
Maximum reaction rate of laccase	14.35 mM.min <sup>-1</sup> [13]
Number of electron	4

transfer at cathode	
Reference potential for anode	-0.32 V [16]
Reference potential for cathode	0.585 V [16]
Conductivity of glassy carbon	8000 S.m <sup>-1</sup> [17,18]
Conductivity of glucose( blood)	10000 S.m <sup>-1</sup> [19]